Report 1170

DEPARTMENT OF THE NAVY

DAVID TAYLOR MODEL BASIN

HYDROMECHANICS

AERODYNAMICS

STRUCTURAL MECHANICS

APPLIED MATHEMATICS

BOUNDARY-LAYER INVESTIGATION ON USS TIMMERMAN (EAG 152) (EX-DD 828)

by

Clifford L. Sayre, Jr.
and
Ralph J. Duerr

HYDROMECHANICS LABORATORY

RESEARCH AND DEVELOPMENT REPORT

August 1960

Report 1170

PRNC-TMB-648 (Rev. 3-58)

BOUNDARY-LAYER INVESTIGATION ON USS TIMMERMAN (EAG 152) (EX-DD 828)

by

Clifford L. Sayre, Jr.
and
Ralph J. Duerr

August 1960

Report 1170
S-F013 08 08

TABLE OF CONTENTS

LIST OF FIGURES

LIST OF TABLES

NOTATION

$C(n)$	Wieghardt coefficient, Equation [10].
$D(x)$	Total drag per unit width
Δh	Manometer reading
k	Pitot-tube calibration coefficient, $u = k\sqrt{2g\Delta h}$
n	Denominator of exponent of power law for velocity profiles, Equation [1]
R_x	Reynolds number, xU_0/ν
U	Potential velocity at outer edge of boundary layer
U_0	Ship velocity
u	Local velocity in boundary layer
v_*	Friction velocity, $\sqrt{\tau_0/\rho}$
x	Distance along centerline of ship from station 0
y	Distance normal to hull surface
δ	Thickness of boundary layer
δ_{FP}	Thickness of flat-plate boundary layer
δ^*	Two-dimensional displacement thickness
η	yv_*/ν
θ	Two-dimensional momentum thickness
ν	Kinematic viscosity of fluid
ρ	Density of fluid
τ_0	Shearing stress at the wall
ϕ	u/v_*

ABSTRACT

Results of velocity measurements in the boundary layer of USS TIMMERMAN (EAG 152) are presented in this report. Measurements of velocities in the throat of the condenser scoop and the pressure drops across the condenser are also given. A generalized form of Prandtl's equation for the growth of the turbulent boundary layer on a flat plate is derived for use in estimating the boundary-layer thickness at large Reynolds numbers.

INTRODUCTION

The design of USS TIMMERMAN (EAG 152) (formerly DD 828) included many innovations in naval and marine engineering. The ship was conceived as a mobile marine experimental facility where new design features could be evaluated. Provision was also made for installing instrumentation and scheduling tests that would provide information applicable to naval architecture and marine engineering, in general. The Bureau of Ships requested[1] that the David Taylor Model Basin design instrumentation for and conduct a flow survey in the vicinity of the condenser scoop and the overboard discharge of the forward main circulating system for a range of ship speeds. Measurements of fluid velocity in the throat of the condenser scoop, pressures, and pressure drops in the condenser and main circulating system were also requested.

These tests had the following objectives:

1. Boundary-layer measurements in the undisturbed flow ahead of the condenser scoop and overboard discharge would provide valuable hydrodynamic data on the nature (i.e., thickness and velocity distribution) of a ship's boundary layer.

2. Measurements of flow direction and velocity in the immediate vicinity of the condenser scoop and overboard discharge would demonstrate the effect (or lack of effect) of these hull openings on the flow around the vessel.

3. The measurements in the throat of the condenser scoop and of pressures and pressure drops in the condenser and main circulating system, could be used along with objectives 1 and 2, to simulate conditions for model tests of condenser circulating system. Such data would also be useful in correlating the results of model tests with full-scale performance.

The tests were conducted during November 1955 in the operating area off Key West, Florida.

---

[1]References are listed on page 18.

INSTRUMENTATION

The velocity and direction of flow in the boundary layer of the destroyer were measured with the specially designed *pitot-static** tubes shown in Figure 1. These pitot tubes were installed at five stations near the scoop and overboard discharge, as shown in Figures 2, 3,

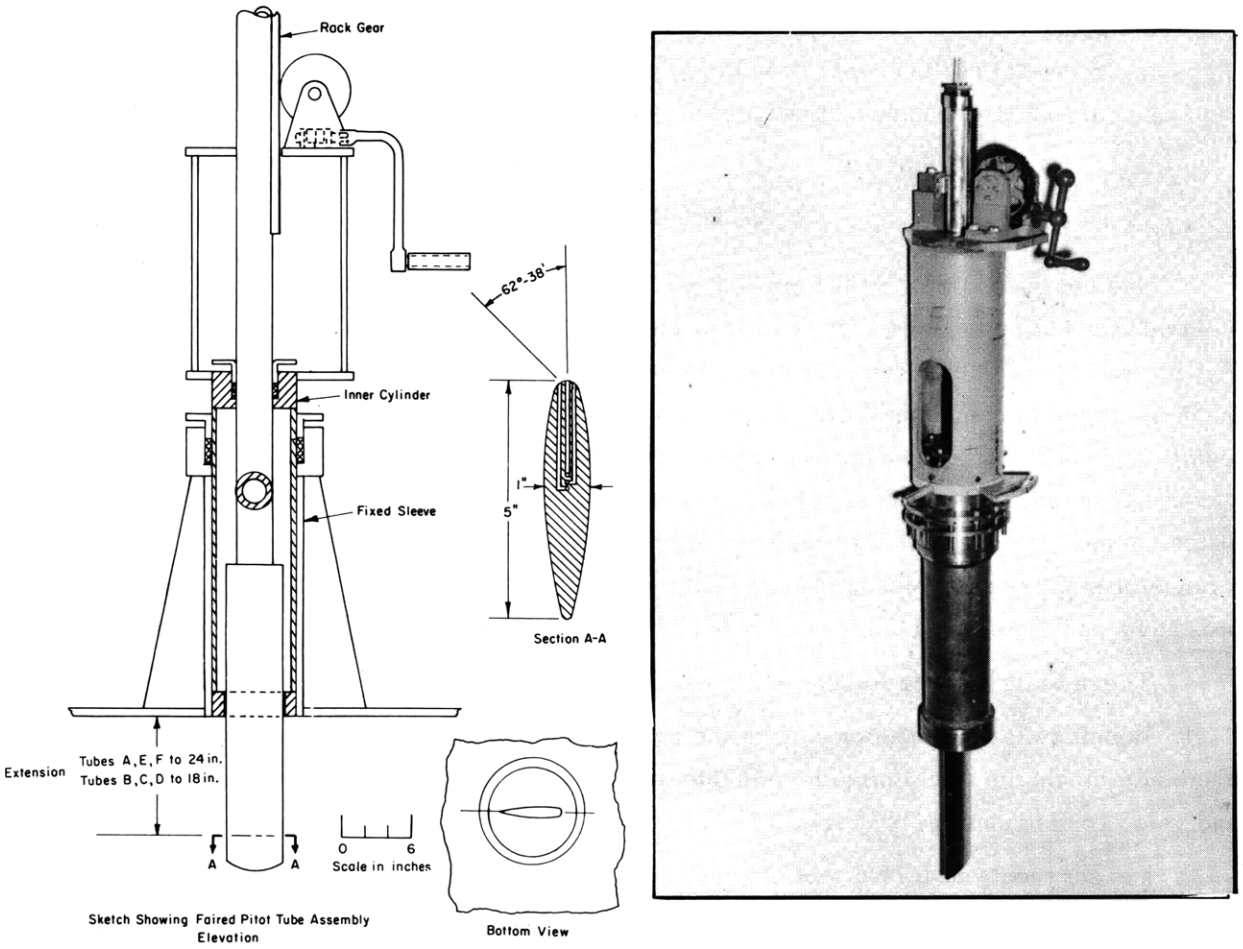

Figure 1 – Pitot Tube for TIMMERMAN Boundary-Layer Survey

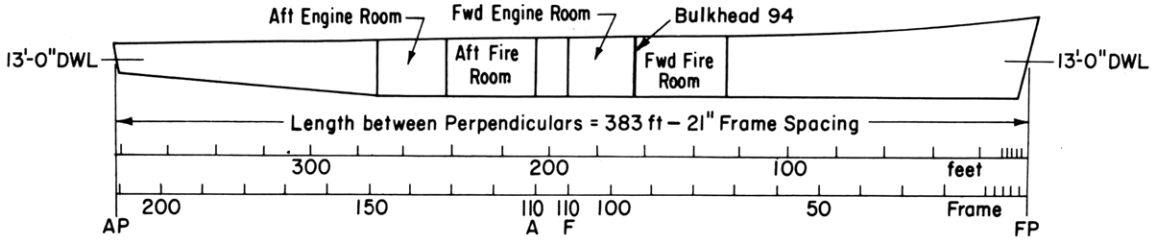

Figure 2 – Inboard Profile of USS TIMMERMAN

*The term *pitot tube* will be used throughout the remainder of this report in place of the more precise *pitot-static tube.*

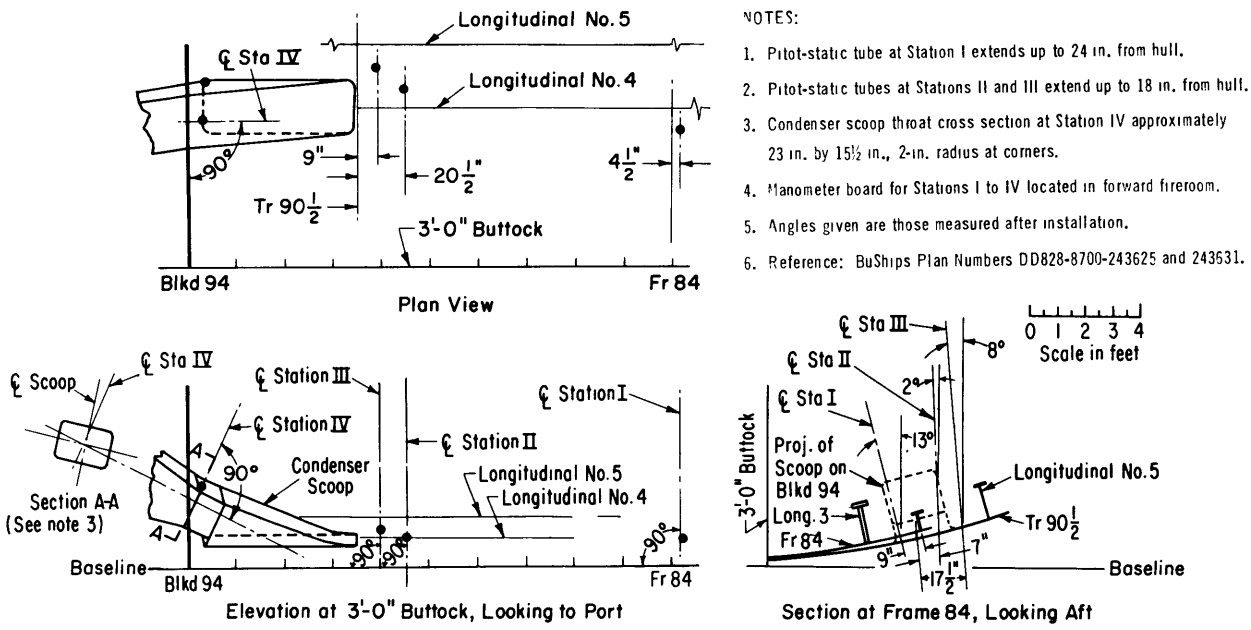

Figure 3 – Pitot-Tube Locations in Forward Fireroom

and 4. The pitot tubes at Stations I, V, and VI could be extended from 0 to 24 inches in a direction approximately normal to the hull surface. The pitot tubes at Stations II and III could be extended from 0 to 18 inches. (Station IV was a conventional Prandtl tube located in the throat of the condenser scoop.) The tangent planes to the hull surface at the measuring stations were approximately parallel to the axis of the vessel. Thus, the pitot tubes were extended in a direction normal to this axis. The direction of flow (in planes perpendicular to the pitot tube) was measured at each extension of the pitot tube by rotating the tube until equal static pressures were obtained at the two static holes. The static pressures were indicated on a manometer located near each of the pitot-tube stations to facilitate making the directional measurements. The flow direction was measured from a line parallel to the center-line of the vessel. After the pitot tube had been aligned with the flow, valves were adjusted to transmit the static pressure and total pressure to a centrally located manometer board. A velocity and direction calibration was made at the Model Basin by mounting the pitot tubes on Towing Carriage 5.

Special back-lighted multiple U-tube manometer boards were used to measure the velocity pressure. One manometer board was located in the forward fireroom and one in the forward engineroom. Tetrabromethane (specific gravity $\simeq 3.0$) was used as a manometer fluid for the 5- and 10-knot measurements. Each manometer board was photographed with a modified Eastman 35mm Recordak camera. The cameras were triggered simultaneously.

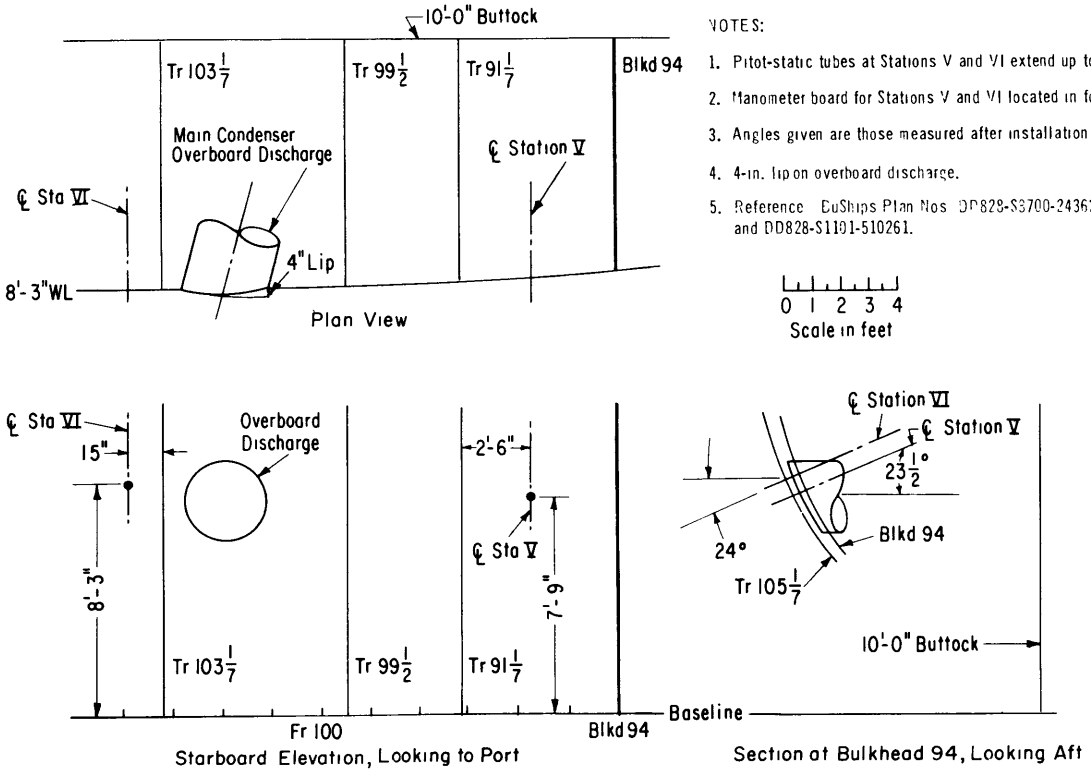

Figure 4 – Pitot-Tube Locations in Forward Engineroom

At Station IV, where the Prandtl tube was located in the throat of the condenser scoop, velocity measurements were obtained along a single vertical line approximating the centerline of the throat, as shown in Figure 3. Additional instrumentation for the condenser, shown in Figure 5, consisted of manometers measuring static pressures and pressure differences in the main circulating system. The manometers for the circulating system were read visually by observers in the engineroom.

BOUNDARY-LAYER SURVEY

OBSERVED RESULTS

The observed data are given in Table 1. Each data point represents the average results of four to eight pictures taken at intervals during a run. The manometer deflections used in computing u were the average values from the photographs corrected for parallax. This correction did not exceed $\pm$ 0.03 inch. The average results compare favorably with the results of observers as recorded in the trial log books.

For the 5- and 10-knot speeds, readings were obtained from both the mercury and tetrabromethane manometers. These results usually agree within 0.1 knot. An estimate of the reproducibility of the results can be obtained by comparing the data for the two series of runs

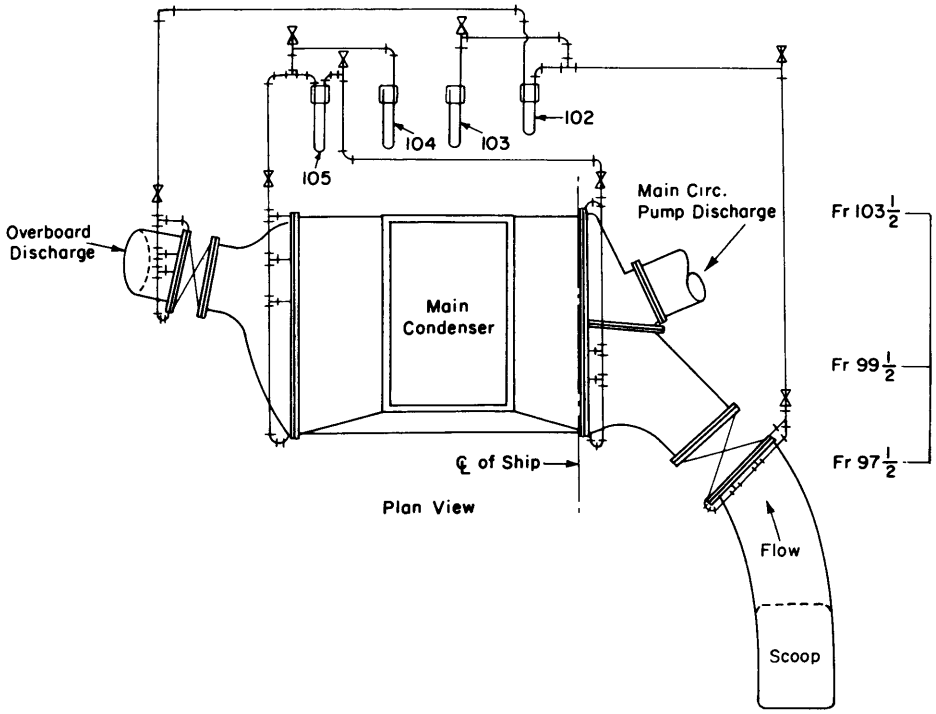

Figure 5 – Schematic Diagram of Condenser Instrumentation

NOTES:

1. All manometer piping 3/8 in. I.P.S.
2. Reference: BuShips Plan Number DD828-8700-243411.

made at 10 knots. For some runs (particularly at Station VI in the separated flow zone aft of the lip of the overboard discharge) a negative manometer deflection occurred. Such readings are entered in Table 1 as **.

The average temperatures prevailing during the tests were:

a. sea water temperature, 78°F; and

b. manometer board temperature, 103°F.

Using these conditions:

$u = k \times 1.871 \sqrt{\Delta h}$ for the tetrabromethane manometers

and

$u = k \times 4.792 \sqrt{\Delta h}$ for the mercury manometers,

where Δh is the manometer reading in inches and u is the velocity in knots.

The ship speed calibration was obtained by measuring revolutions over the trial course just prior to the boundary-layer survey runs. Speeds given for individual runs are probably accurate within $\pm$ 0.10 knot.

TABLE 1

Observed Boundary-Layer Data

Station	y inches	U_0 knots	Angle degrees	u/U_0 mercury manometer	u/U_0 tetrabromethane manometer	U_0 knots	Angle degrees	u/U_0 mercury manometer	u/U_0 tetrabromethane manometer	U_0 knots	Angle degrees	u/U_0 mercury manometer	u/U_0 tetrabromethane manometer	U_0 knots	Angle degrees	u/U_0 mercury manometer	U_0 knots	Angle degrees	u/U_0 mercury manometer
I	0.125	4.8	0	0.494	0.488	10.3	0	0.538	0.534	10.6	0	0.528	0.530	15.3	0	0.585	19.7	0	0.567
I	0.25	4.6	0	0.562	0.574	10.4	0	0.583	0.579	10.6	0	0.563	0.567	15.3	0	0.630	19.4	0	0.639
I	0.50	4.8	0	0.632	0.619	10.3	0	0.637	0.635	10.6	0	0.595	0.601	15.3	0	0.675	19.6	0	0.660
I	0.75	5.0	0	0.585	0.583	10.4	0	0.640	0.632	10.4	0	0.659	0.659	15.2	0	0.702	19.9	0	0.711
I	1.00	4.8	0	0.639	0.633	10.2	0	0.660	0.656	10.4	0	0.691	0.684	15.2	0	0.721	19.8	0	0.716
I	2.00	4.7	0	0.668	0.684	10.6	0	0.707	0.706	10.5	0	0.731	0.736	15.2	1 P	0.765	19.7	1	0.719
I	4.00	4.7	0	0.688	0.709	10.8	0	0.791	0.791	10.6	0	0.778	0.779	15.3	2 P	0.796	19.8	0	0.808
I	7.00	4.7	0	0.786	0.803	10.6	0	0.725	0.729	10.4	0	0.831	0.830	15.3	¾ P	0.857	19.8	0	0.848
I	10.0	4.7	0	0.839	0.855	10.8	0	0.881	0.881	10.7	0	0.881	0.882	15.3	1½ P	0.940	19.6	0	0.893
I	13.0	4.8	2 P	0.870	0.870	10.7	0	0.903	0.905	10.4	0	0.943	0.948	15.3	1½ P	0.958	19.8	0	0.935
I	16.0	4.9	2 P	0.903	0.906	10.7	0	0.922	0.924	10.5	0	0.960	0.964	15.3	1½ P	0.969	20.0	0	0.945
I	19.0	4.8	2 P	0.902	0.897	10.7	0	0.977	0.983	10.4	0	0.962	0.981	15.2	1 P	0.988	19.9	0	1.004
I	24.0	4.6	–	0.919	0.914	10.3	0	0.999	1.004	10.4	0	0.993	0.999	15.3	1 P	0.984	19.8	0	1.005
II	0.125	4.8	1	0.471	0.544	10.3	1 S	0.557	0.570	10.6	1½ P	0.605	0.645	15.3	1 S	0.637	19.7	1 P	0.570
II	0.25	4.6	1	0.559	0.626	10.4	1 S	0.578	0.596	10.6	1½ P	0.609	0.653	15.3	1 S	0.668	19.4	1 S	0.658
II	0.50	4.8	1	0.661	0.694	10.3	1 S	0.653	0.662	10.6	2 P	0.657	0.690	15.3	1 S	0.679	19.6	1 S	0.664
II	0.75	5.0	1	0.648	0.683	10.4	1 S	0.648	0.657	10.4	1 P	0.732	0.717	15.2	1 S	0.745	19.9	1 S	0.706
II	1.00	4.8	1	0.682	0.716	10.2	1 S	0.688	0.698	10.4	1 P	0.758	0.749	15.2	1 S	0.751	19.8	1 S	0.756
II	2.00	4.7	1	0.744	0.770	10.6	1 S	0.791	0.803	10.5	1 P	0.759	0.767	15.2	1 S	0.831	19.7	1 S	0.759
II	4.00	4.7	–	0.795	0.823	10.8	1 S	0.831	0.842	10.6	1 P	0.814	0.797	15.3	1 P	0.846	19.8	1 S	0.848
II	7.00	4.7	–	0.892	0.938	10.6	1 S	0.700	0.705	10.4	1 P	0.809	0.840	15.3	1 P	0.869	19.8	1 S	0.857
II	10.0	4.7	–	0.938	0.978	10.8	1 S	0.912	0.922	10.7	1 P	0.874	0.867	15.3	1 P	0.932	19.6	1 S	0.882
II	13.0	4.8	–	0.924	0.956	10.7	1 S	0.922	0.935	10.4	1 P	0.931	0.935	15.3	1 P	0.971	19.8	1 S	0.967
II	16.0	4.9	–	0.959	0.981	10.7	1 S	0.958	0.967	10.5	1 P	0.928	0.942	15.3	1 P	0.974	20.0	1 S	0.956
II	18.0	4.8	–	0.969	1.003	10.7	1 S	1.008	1.007	10.4	1 P	0.972	0.964	15.2	1 P	0.976	19.9	1 S	1.032
III	0.125	4.8	1¼ P	**	**	10.3	1¼	0.538	0.543	10.6	1¼ P	0.472	0.471	15.3	1¼ P	0.605	19.7	1¼ P	0.625
III	0.25	4.6	1¼ P	0.141	0.156	10.4	1¼	0.545	0.548	10.6	1¼ P	0.494	0.492	15.3	1¼ P	0.659	19.4	1¼ P	0.656
III	0.50	4.8	1¼ P	0.345	0.367	10.3	1¼	0.594	0.596	10.6	1¼ P	0.484	0.492	15.3	1¼ P	0.682	19.6	1¼ P	0.685
III	0.75	5.0	1¼ P	0.356	0.375	10.4	1¼	0.612	0.612	10.4	1¼ P	0.548	0.550	15.2	1¼ P	0.722	19.9	1¼ P	0.700
III	1.00	4.8	1¼ P	0.383	0.422	10.2	1¼	0.643	0.643	10.4	1¼ P	0.565	0.567	15.2	1¼ P	0.756	19.8	1¼ P	0.745
III	2.00	4.7	1¼ P	0.469	0.492	10.6	1¼	0.697	0.699	10.5	1¼ P	0.596	0.591	15.3	1¼ P	0.796	19.7	1¼ P	0.751
III	4.00	4.7	1¼ P	0.509	0.541	10.8	1¼	0.755	0.757	10.6	1¼ P	0.652	0.651	15.3	1¼ P	0.834	19.8	1¼ P	0.834
III	7.00	4.7	1¼ P	0.619	0.649	10.6	1¼	0.687	0.689	10.4	1¼ P	0.705	0.709	15.3	1¼ P	0.915	19.8	1¼ P	0.852
III	10.0	4.7	1¼ P	0.679	0.696	10.8	1¼	0.853	0.854	10.7	1¼ P	0.757	0.756	15.3	1¼ P	0.980	19.6	1¼ P	0.862
III	13.0	4.8	1¼ P	0.665	0.682	10.7	1¼	0.876	0.878	10.4	1¼ P	0.819	0.822	15.3	1¼ P	0.991	19.8	1¼ P	0.943
III	16.0	4.9	1¼ P	0.684	0.704	10.7	1¼	0.893	0.894	10.5	1¼ P	0.823	0.826	15.3	1¼ P	0.990	20.0	1¼ P	0.891
III	18.0	4.8	1¼ P	0.692	0.714	10.7	1¼	0.923	0.926	10.4	1¼ P	0.847	0.851	15.2	1¼ P	0.999	19.9	1¼ P	0.972
III	18.0	4.6	1¼ P	0.730	0.741	10.3	1¼	0.944	0.949								19.8	1¼ P	0.978
V	0.125	4.8	0	0.529	0.436	10.3		0.524	0.521	10.6	1 D	0.593	0.520	15.3	0	0.598	19.7	0	0.637
V	0.25	4.6	0	0.560	0.476	10.4		0.589	0.583			**	**	15.3	0	0.674	19.4	0	0.705
V	0.50	4.8	0	0.731	0.680	10.3		0.590	0.588	10.6	1 D	0.658	0.589	15.3	0	0.685	19.6	0	0.734
V	0.75	5.0	0	0.713	0.663	10.4		0.598	0.602	10.4	1 D	0.704	0.634	15.2	0	0.717	19.9	0	0.741
V	1.00	4.8	0	0.708	0.656	10.2		0.667	0.660	10.4	1 D	0.708	0.635	15.2	2 D	0.783	19.8	0	0.750
V	2.00	4.7	0	0.735	0.690	10.6		0.717	0.714	10.5	3 D	0.768	0.714	15.2	2 D	0.821	19.7	½ D	0.825
V	4.00	4.7	0	0.729	0.665	10.8		0.833	0.827	10.6	1 D	0.815	0.762	15.3	2 D	0.889	19.8	1½ D	0.878
V	7.00	4.7	0	0.842	0.800	10.6		0.868	0.864	10.4	1 D	0.894	0.852	15.3	2 D	0.984	19.8	1 D	0.920
V	10.0	4.7	0	0.904	0.860	10.8		0.937	0.882	10.7	2 D	0.933	0.901	15.3	2 D	0.966	19.6	1 D	1.017
V	13.0	4.8	0	0.885	0.845	10.7		0.967	0.938	10.4	1 D	0.981	0.946	15.3	2 D	1.010	19.8	1 D	1.022
V	16.0	4.9	0	0.876	0.830	10.7		0.981	0.938	10.5	1 D	0.938	0.952	15.3	2.5 D	0.979	20.0	1 D	1.022
V	19.0	4.8	0	0.918	0.879	10.7		0.958	0.938	10.4	1 D	0.957	0.961	15.2	2.5 D	0.991	19.9	1 D	1.017
V	24.0	4.6	0	0.810	0.791	10.3		0.989	0.974	10.4	2	0.932	0.961	15.3	2.5 D	0.941	19.8	1 D	1.009
VI	0.125			**	**			**	**	10.6	0	0.279	0.376			**			**
VI	0.25			↓	↓			↓	↓			**	**			↓			↓
VI	0.50									10.6	0	0.192	0.355						
VI	0.75									10.4	0	0.225	0.369						
VI	1.00									10.4	0	0.144	0.317						
VI	2.00									10.5	0	0.230	0.382	15.2	0	0.250			
VI	4.00									10.6	0	0.153	0.354			**	19.8	0	0.151
VI	7.00									10.4	0	0.225	0.393			↓			**
VI	10.0	4.7	0	0.276	0.131	10.8	0	0.694	0.613	10.7	6 S	0.417	0.502						**
VI	13.0	4.8	0	0.636	0.609	10.7	0	0.507	0.508	10.4	4½ S	0.509	0.580	15.3	0	0.333	19.8	0	0.270
VI	16.0	4.9	0	0.703	0.703	10.7	0	0.770	0.770	10.5	1½ S	0.720	0.762	15.3	0	0.707	20.0	0	0.643
VI	19.0	4.8	0	0.787	0.805	10.7	0	0.960	0.966	10.4	½ S	0.918	0.912	15.2	0	0.948	19.9	0	0.983
VI	24.0	4.6	0	0.724	0.722	10.3	0	1.024	1.026	10.4	0	0.946	0.946	15.3	0	0.985	19.8	0	1.084

**Negative manometer deflection

DISCUSSION OF RESULTS

The ship speed U_0 was used in plotting the velocity profiles in Figure 6 because the data did not show a potential velocity U perceptibly different from U_0. The velocity profiles are of the generalized parabolic shape. The only profiles showing unusual characteristics are those at Station VI, which was located downstream of the overboard discharge. These plots indicate a region of separation (probably caused by the lip on the overboard discharge), and show the jet of fluid injected into this region by the overboard discharge. The velocity profiles for Station VI are shown in Figure 6 and the data are given in Table 1, but no boundary-layer parameters were calculated for this location because of the irregular nature of the flow.

A curve-fitting technique[2] was used to find the values of δ and n given in Table 2, with the assumption that the velocity profile was of the form

$$\frac{u}{U_0} = (y/\delta)^{1/n}. \qquad [1]$$

Except for the 5-knot condition, the values of δ obtained are in quantitative agreement with the small amount of existing data for corresponding Reynolds numbers.[3,4]

The expression for displacement thickness

$$\delta^* = \int_0^y \left(1 - \frac{u}{U}\right) dy, \qquad [2]$$

can be used to obtain δ^* by graphical integration of the velocity profiles. Substituting Equation [1] into Equation [2] and integrating from $y = 0$ to $y = \delta$ gives

$$\delta^* = \frac{1}{n+1}\,\delta. \qquad [3]$$

Alternative estimates of δ which are tabulated as $\delta(\delta^*)$ were obtained using values of n from the numerical analysis and values of δ^* from the graphical integration in Equation [3].

The momentum thickness

$$\theta = \int_0^y \frac{u}{U}\left(1 - \frac{u}{U}\right) dy \qquad [4]$$

was also determined graphically from the experimental points and is given in Table 2.

The values of n obtained show the effect of increasing Reynolds number, and are in substantial agreement with the values given in Reference 3 for full-scale measurements on the merchant ship SNAEFELL. These values also show agreement with extrapolated values of n for the tests on friction planes reported in Reference 5. Schlichting[6] also corroborates the increase of n with increasing Reynolds number for pipes.

(Text continued on page 11.)

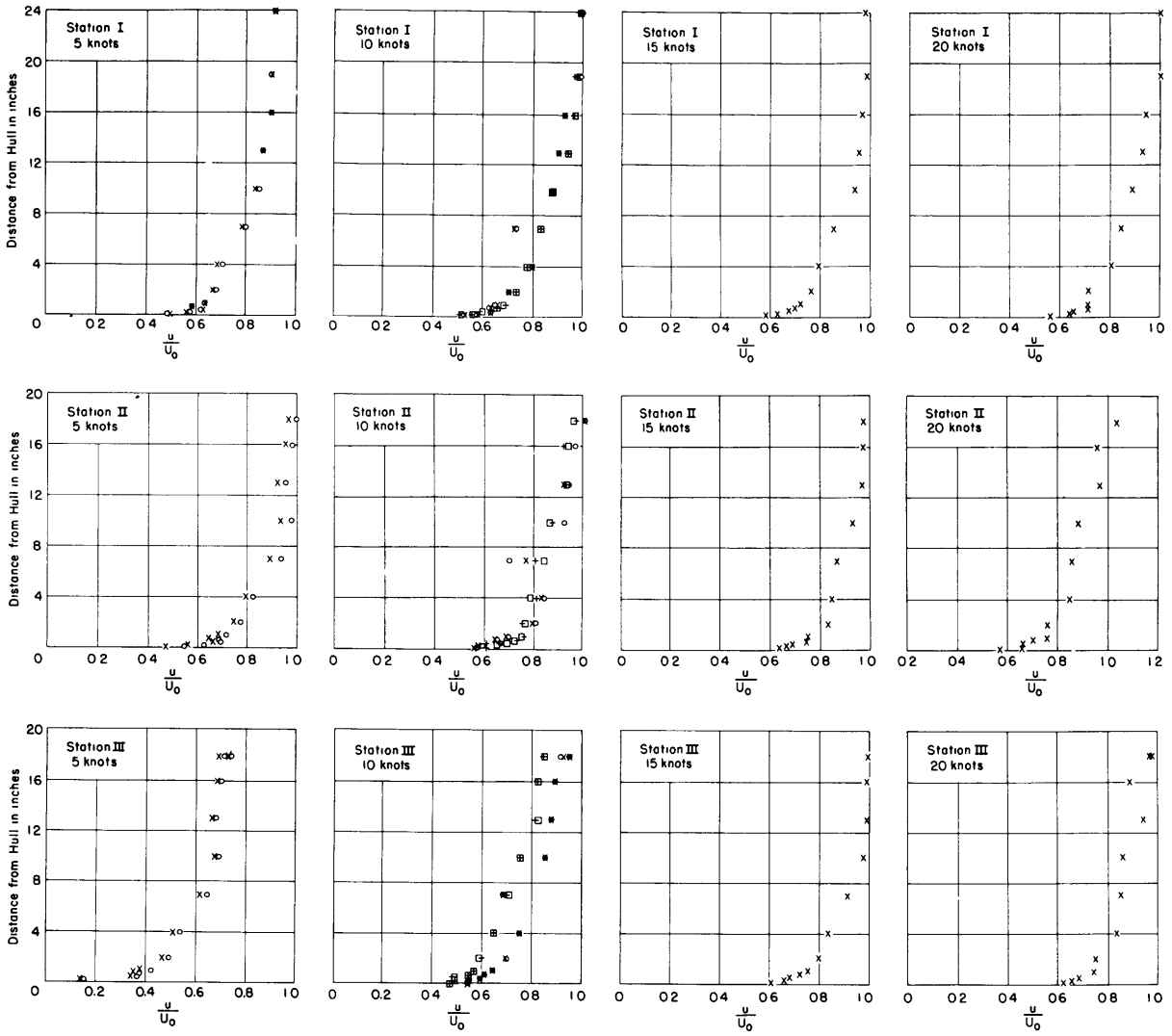

Figure 6a

○ □ = Mercury Manometer

\+ x = Tetrabromethane Manometer

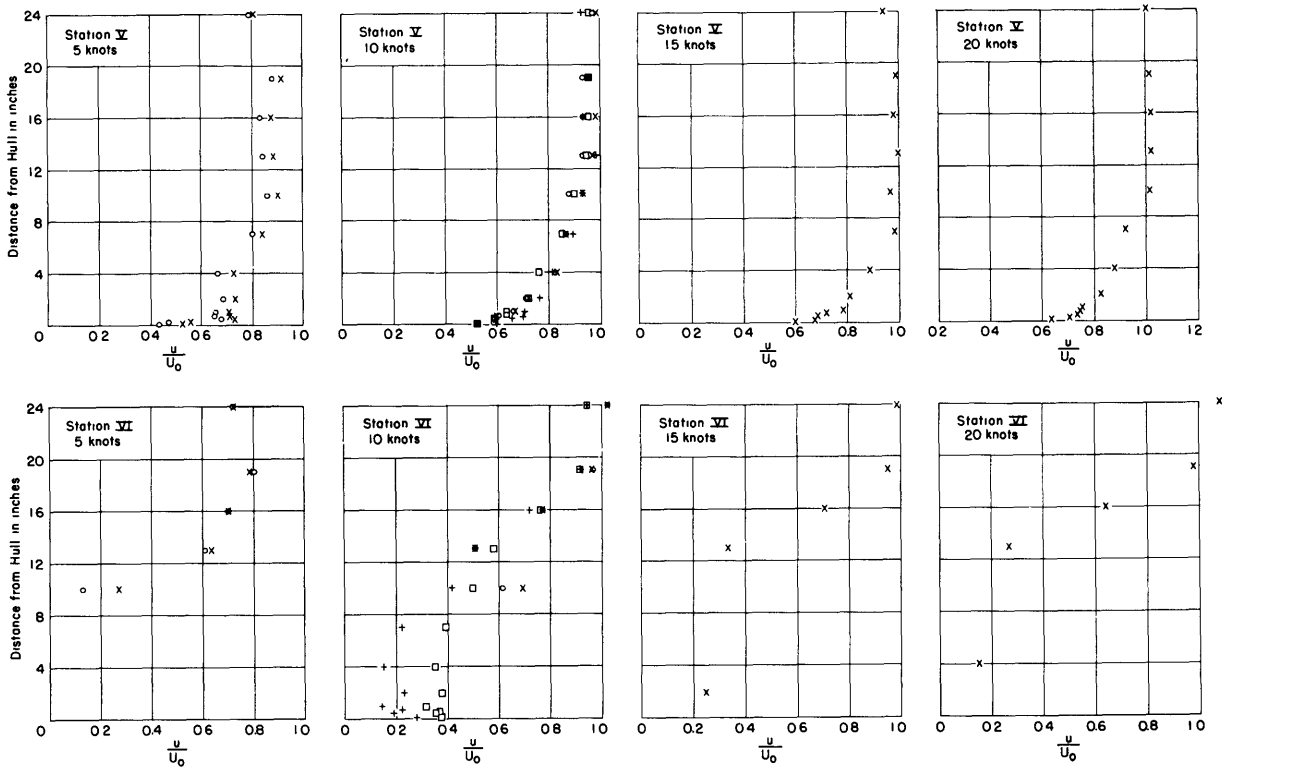

Figure 6b

Figure 6 – Boundary-Layer Velocity Profiles at Stations I, II, III, V, and VI

TABLE 2

Computed Boundary-Layer Data

Station	x feet	U_0 knots	R_x $\times 10^{-8}$	n	δ inches	δ^* inches	$\delta(\delta^*)$ inches	θ inches	(1) δ_{FP} inches
I	146.7	5	1.24	8.59	48	–	–	–	20
↓	↓	10	2.49	8.47	28	2.73	26	2.14	19
		10	2.49	8.05	24	2.73	25	2.14	19
		15	3.74	9.74	24	2.18	23	1.79	19
↓	↓	20	4.98	9.78	28	2.57	28	2.04	18
II	156.7	5	1.33	8.39	16	1.61	15	1.34	22
↓	↓	10	2.66	8.87	22	2.46	24	1.99	20
		10	2.66	12.29	43	2.46	33	1.99	20
		15	3.99	11.08	23	1.98	24	1.72	20
↓	↓	20	5.32	9.79	22	2.20	24	1.84	20
III	157.6	5	1.34	5.05	80	–	–	–	22
↓	↓	10	2.68	8.76	43	–	–	–	21
		10	2.68	–	–	–	–	–	21
		15	4.02	9.60	16	1.54	16	1.26	20
↓	↓	20	5.36	11.88	41	2.27	29	1.88	20
V	167.5	5	1.42	8.21	48	–	–	–	23
↓	↓	10	2.84	8.03	27	3.07	28	2.55	22
		10	2.84	8.07	28	3.07	28	2.55	22
		15	4.26	9.86	16	1.28	14	1.10	21
↓	↓	20	5.68	10.53	15	1.37	16	1.14	21

[1] δ_{FP} from Equation [6].

The measurements of flow angles show that the flow was essentially parallel to the direction of motion of the ship in the regions investigated.

ESTIMATING THE THICKNESS OF THE BOUNDARY LAYER

The Prandtl or Von Karman formula is often used to estimate the growth of the turbulent boundary layer along a smooth flat plate:

$$\delta_{FP} = 0.37\ x\ R_x^{-0.2} \qquad [5]$$

However, Equation [5] was derived on the basis of $n = 7$ in Equation [1] and hence is valid for only a limited range of Reynolds numbers. To determine whether δ_{FP} would provide a useful engineering estimate for the magnitude of δ on a ship a general expression was derived for δ_{FP} as a function of n. (See Appendix.)

$$\delta_{FP}\ (x, n) = \left[\frac{(2+n)(3+n)}{n}\right]^{\frac{n+1}{3+n}} \left[\frac{1}{C(n)}\right]^{\frac{2n}{3+n}} x\ R_x^{-\frac{2}{3+n}} \qquad [6]$$

$C(n)$ is a dimensionless empirical coefficient related to the friction velocity. The values of $C(n)$, shown in Table 3, are given in Reference 6, as obtained from an analysis of experimental data by Wieghardt.

TABLE 3

Values of $C(n)$

n	7	8	9	10
$C(n)$	8.74	9.71	10.6	11.5

Equation [5] then becomes a special case of Equation [6] for $n = 7$. Values of n were obtained as a function of Reynolds number for Figure 7 from Landweber's data.[7] Values of δ_{FP} computed from Equation [6], using values of n from Figure 7 and $C(n)$ from Figure 8, are also given in Table 2.

The variation of $C(n)$ and n with Reynolds number, together with Equation [6], explains the difficulty of detecting a variation in δ with ship speed, as experienced by Baker[3] and Allan.[5] At high Reynolds numbers the simultaneous changes in $C(n)$ and n occur in different directions, giving an apparent relationship

$$\delta \simeq K\ x \qquad [7]$$

where K is a constant.

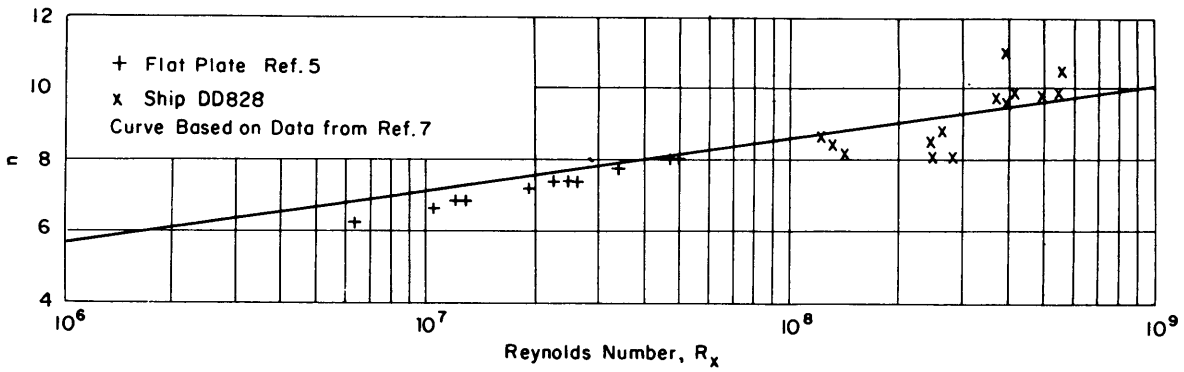

Figure 7 – Variation of Velocity Profiles Exponent with Reynolds Number

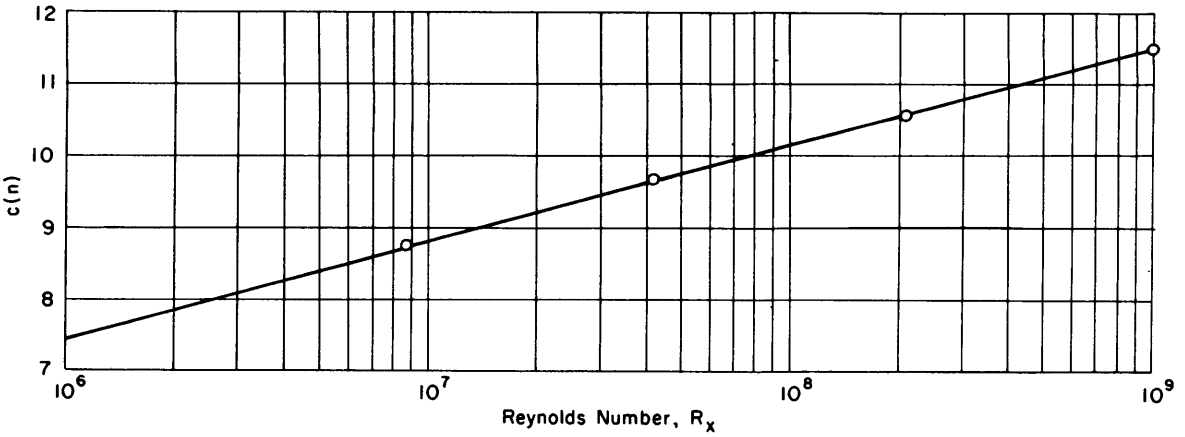

Figure 8 – Variation of $C(n)$ with Reynolds Number

The use of Equation [6] (or similar relationship) for approximating the growth of the boundary layer on a ship is often necessary because of the paucity of full-scale measurements. Strictly speaking, Equation [6] is applicable to only the two-dimensional turbulent flow over a smooth flat plate in the absence of a pressure gradient. However, much of the hull surface is flat, or relatively so; and in many of these regions the longitudinal pressure gradient is small. In such cases the use of Equation [6] will give a more realistic estimate of δ than will Equation [5]. Values of n and $C(n)$ to be used in Equation [6] are given in Figures 7 and 8, respectively.

MAIN-CIRCULATING-SYSTEM MEASUREMENTS

The velocity profiles measured in the throat of the condenser scoop are plotted in Figure 9 and given in Table 4. The flow rates in Figure 10a were computed by assuming that the flow in the throat was two-dimensional. The flow rate versus ship speed is plotted in Figure 10a. The dotted line represents an extrapolation to the design condition at 38 knots. Figure 10a shows that the flow through the condenser varies as the 1.3 power of the ship velocity. This variation is possible since the scoop receives water from the boundary layer where the kinetic energy is less than in the free stream.

The pressure differences across portions of the main circulating system are plotted in Figure 10b. The wide scatter of points is due in part to the large changes in the manometer readings which occurred during runs. Part of the error may also be due to recording errors by observers and to the difficulty of visually averaging the fluctuations. The condenser measurements were requested subsequent to the initial planning, too late to provide a unified installation which could be photographed in the manner of the boundary-layer survey manometers. The fairing used in Figure 10b was chosen to use the maximum number of data points consistent with making the head loss curves approximately parallel. This choice of fairing shows the pressure losses in the system to be directly proportional to the rate of flow through the condenser. Dimensional analysis and data on friction losses in piping systems show that the head loss should be proportional to the square of the flow rate (i.e., the square of the velocity through the system). Friction losses in the tubes and water boxes were calculated from data in Reference 8 and plotted on Figure 10b for comparison. A recent paper by Dudley[9] gives a comprehensive series of measurements on a destroyer-type vessel.

CONCLUSIONS

The shape of the velocity profiles measured in the boundary layer of the destroyer is similar to the shape of velocity profiles measured in the boundary layer of a flat plate at the same Reynolds number. The thicknesses of the ship boundary layer and flat-plate boundary layer are approximately the same at the same Reynolds number. Equation [6] provides a better estimate of the boundary-layer thickness than does the Prandtl formula. The data on the internal performance of the main circulating system are not accurate enough nor consistent enough to provide a basis for significant conclusions about the performance of the condenser.

ACKNOWLEDGMENTS

The data forming the basis of this report were obtained by personnel of the Flow Studies Section, under the general guidance and direction of Mr. M.S. Macovsky.

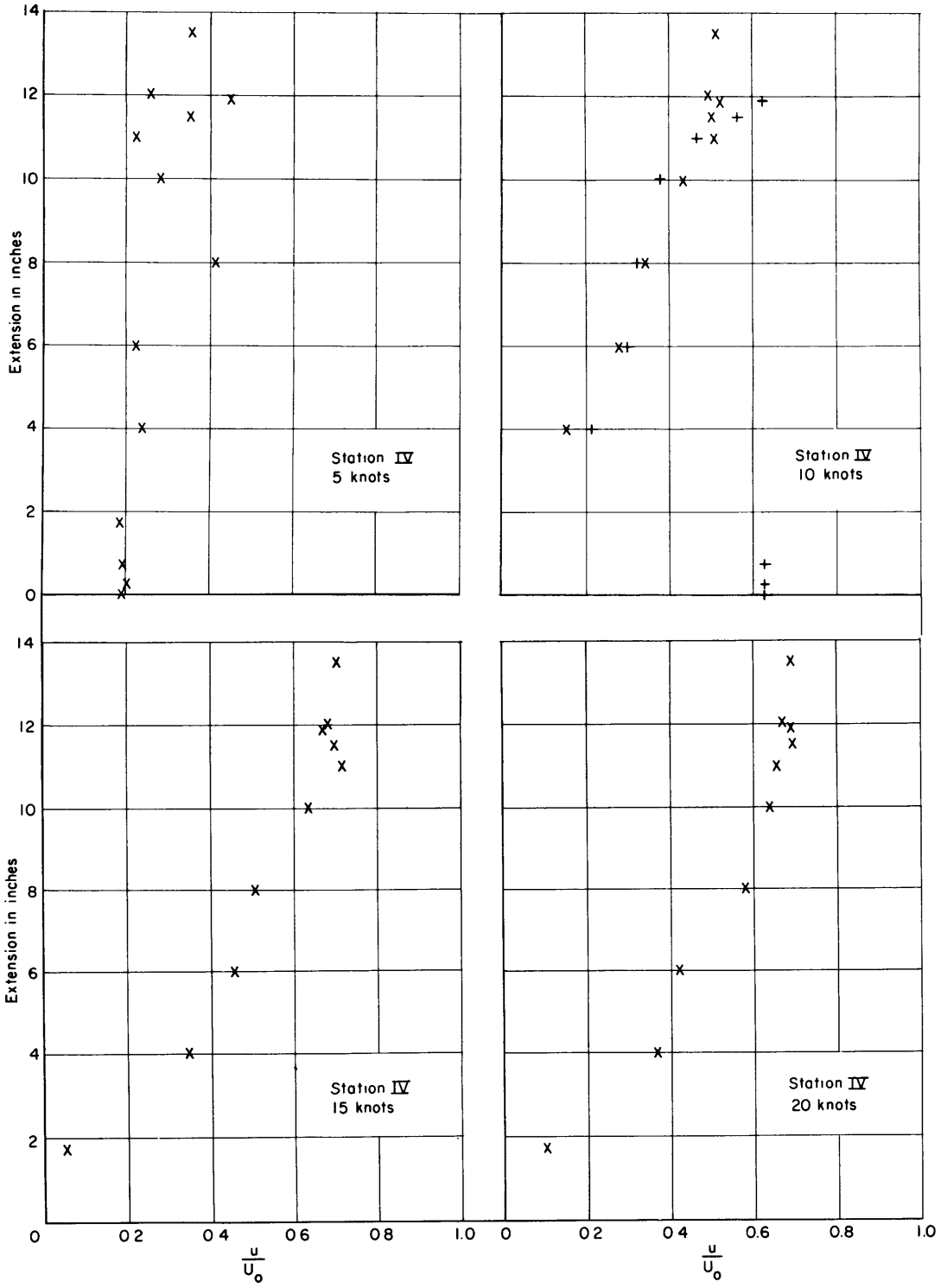

Figure 9 – Velocity Profiles in Throat of Condenser Scoop

TABLE 4 – Condenser Scoop Throat Data

IV	y	U_0	u/U_0	U_0	u/U_0	U_0	u/U_0	U_0	u/U_0	U_0	u/U_0
	0	4.8	0.1963		**	10.6	0.6278		**		**
	0.25	4.6	0.2048		↓	10.6	0.6278		↓		↓
	0.75	4.8	0.1963			10.6	0.6278				
	1.75	5.0	0.1884				**	15.2	0.0536	19.9	0.1006
	4	4.8	0.2404	10.2	0.1532	10.4	0.2129	15.2	0.3468	19.8	0.3574
	6	4.7	0.2241	10.6	0.2789	10.5	0.2994	15.2	0.4541	19.7	0.4202
	8	4.7	0.4137	10.8	0.3438	10.6	0.3227	15.3	0.5056	19.8	0.5791
	10	4.7	0.2835	10.6	0.4342	10.4	0.3801	15.3	0.6348	19.8	0.6467
	11	4.7	0.2241	10.8	0.5103	10.7	0.4671	15.3	0.7150	19.6	0.6552
	11.5	4.8	0.3542	10.7	0.5027	10.4	0.5631	15.3	0.6989	19.8	0.6943
	11.875	4.9	0.4518	10.7	0.5233	10.5	0.6240	15.3	0.6703	20.0	0.6884
	12	4.8	0.2596	10.7	0.4926		**	15.2	0.6878	19.9	0.6707
	13.5	4.6	0.3551	10.3	0.5118		**	15.3	0.7048	19.8	0.6896

**Negative manometer deflections

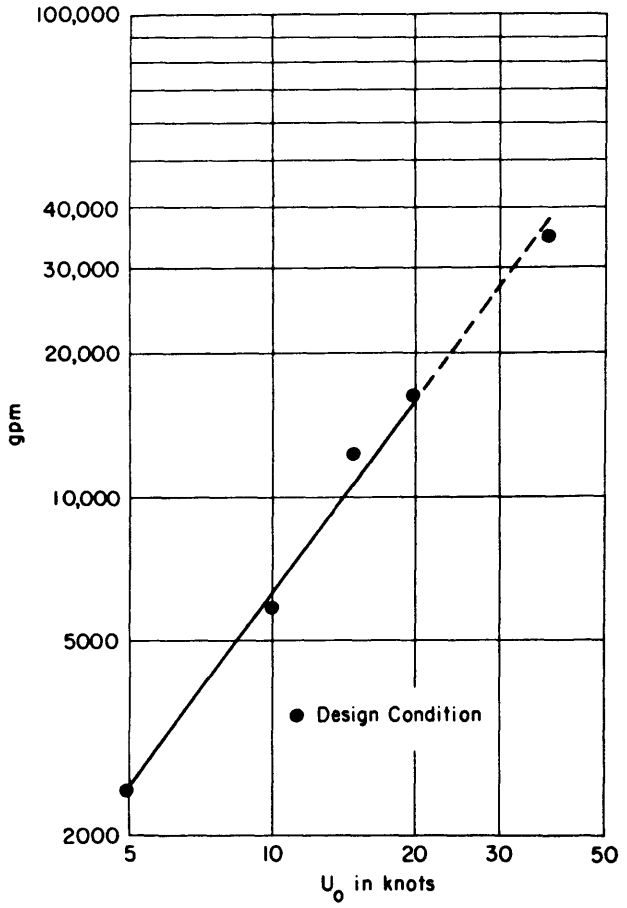

Figure 10a

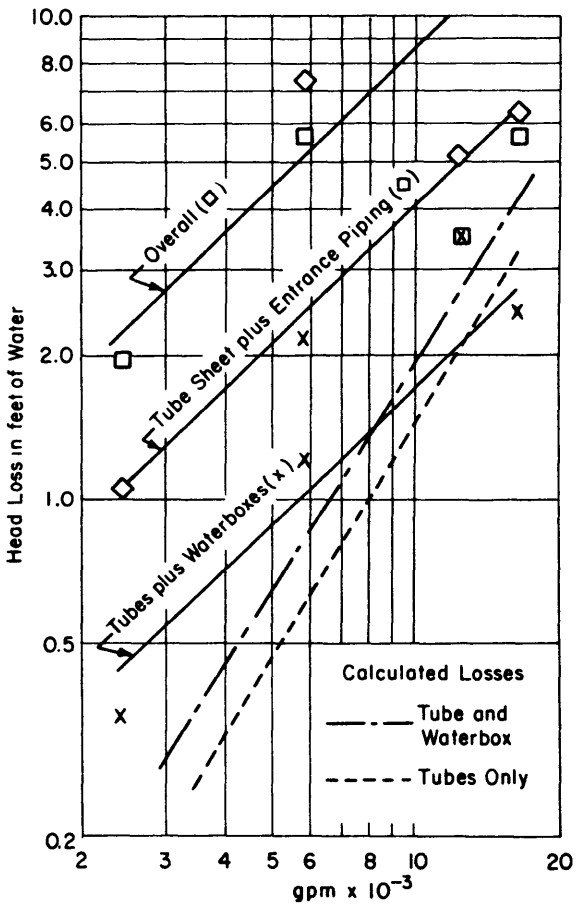

Figure 10b

Figure 10 – Circulating System Performance Curves

APPENDIX

DERIVATION OF EQUATION [6]

Using the definitions

$$\phi = \frac{u}{v_*} \qquad [8]$$

and

$$\eta = \frac{y v_*}{\nu} \qquad [9]$$

Wieghardt[6] assumed

$$\phi = C(n)\,\eta^{\frac{1}{n}}. \qquad [10]$$

From an analysis of experimental results, he obtained the data given in Table 3.
Substituting Equations [8] and [9] in [10], we can obtain

$$v_*^2 = \left[\frac{u}{C(n)}\right]^{\frac{2n}{n+1}} \left[\frac{\nu}{y}\right]^{\frac{2}{n+1}} \qquad [11]$$

which gives

$$v_*^2 = \left[\frac{u_0}{C(n)}\right]^{\frac{2n}{n+1}} \left[\frac{\nu}{\delta}\right]^{\frac{2}{n+1}} \qquad [11a]$$

for $u = u_0$ at $y = \delta$.
Now, the drag per unit width is

$$D(x) = \int_0^x \tau_0(x)\,dx = \rho \int_0^\delta u\,(U_0 - u)\,dy, \qquad [12]$$

and the momentum thickness is

$$\theta U_0^2 = \int_0^\delta u\,(U_0 - u)\,dy. \qquad [4]$$

Substituting Equation [4] in [12] and differentiating the resulting equation with respect to x gives

$$\frac{d}{dx}\,D(x) = \tau_0(x) = \rho\,U_0^2\,\frac{d\theta}{dx}\,. \qquad [13]$$

But

$$\tau_0 = \rho\,v_*^2. \qquad [14]$$

Integrating Equation [4], we get

$$\frac{\theta}{\delta} = \frac{n}{(1+n)\,(2+n)}. \qquad [15]$$

Combining Equation [15] with

$$\delta^* = \frac{1}{n+1}\,\delta \qquad [3]$$

and substituting in Equation [13] gives

$$\frac{\tau_0(x)}{\rho\, U_0^2} = \frac{n}{(1+n)(2+n)}\,\frac{d\delta}{dx} = \left[\frac{1}{C(n)}\right]^{\frac{2n}{n+1}} \left[\frac{\nu}{U_0\,\delta}\right]^{\frac{2}{n+1}} \qquad [16]$$

Assuming $\delta = 0$ at $x = 0$ and integrating, we get:

$$\delta(x) = \left[\frac{(2+n)(3+n)}{n}\right]^{\frac{n+1}{3+n}} \left[\frac{1}{C(n)}\right]^{\frac{2n}{3+n}} \left[\frac{\nu}{U_0 x}\right]^{\frac{2}{3+n}} x \qquad [6a]$$

$$= \left[\frac{(2+n)(3+n)}{n}\right]^{\frac{n+1}{3+n}} \left[\frac{1}{C(n)}\right]^{\frac{2n}{3+n}} \left[\frac{1}{R_x}\right]^{\frac{2}{3+n}} x \qquad [6]$$

A result similar to Equation [6a] was obtained by Schoenherr.[10]

REFERENCES

1. Bureau of Ships letter DD828/S8 (436); EM8/A2-6 Serial 436-136 of 27 Apr 1953 to David Taylor Model Basin.

2. Wylie, C.R., "Advanced Engineering Mathematics," McGraw-Hill, New York (1951) p. 533.

3. Baker, G.S., "Ship Wake and the Frictional Belt," Transactions, North-East Coast Institution of Engineers and Shipbuilders, Vol. 46 (1929-30) pp. 83-106.

4. Breslin, J.P. and Ellsworth, W.M., Jr., "Progress Report Research on Main Injection Scoops and Overboard Discharges," David Taylor Model Basin Report 793 (Sep 1951).

5. Allan, J.F. and Cutland, R.S., "Wake Studies of Plane Surfaces," Transactions, North-East Coast Institution of Engineers and Shipbuilders, Vol. 69 (1952-53) pp. 245-266.

6. Schlichting, H., "Boundary Layer Theory," McGraw-Hill, New York (1955) Chapter XX.

7. Landweber, L., "The Frictional Resistance of Flat Plates in Zero Pressure Gradient," Transactions, Society of Naval Architects and Marine Engineers, Vol. 61 (1953) p. 16.

8. Gaffert, G.A., "Steam Power Stations," McGraw-Hill, New York (3rd ed. 1946), Chapter 4.

9. Dudley, S.A., "Flow Characteristics of Main Condenser Scoop Injection System Based on Shipboard Tests," paper read before New England Section, Society of Naval Architects and Marine Engineers (May 1958).

10. Schoenherr, Karl E., "Resistance of Flat Surfaces," Transactions, Society of Naval Architects and Marine Engineers, Vol. 40 (1932) p. 282, Equation [11].

INITIAL DISTRIBUTION

Copies	
11	CHBUSHIPS 3 Tech Info Br (Code 335) 1 Tech Asst (Code 106) 1 Appl Sci (Code 340) 1 Ship Des (Code 410) 1 Prelim Des (Code 420) 2 Mach, Sci & Res (Code 436) 2 Heat Exchangers (Code 651C)
4	CHBUWEPS(R) 2 RAAD-3
4	CHONR 2 Fluid Dyn (Code 438)
1	NAVSHIPYD BSN
1	NAVSHIPYD CHASN
1	NAVSHIPYD MARE
1	NAVSHIPYD NORVA
1	NAVSHIPYD NYK
1	NAVSHIPYD PEARL
1	NAVSHIPYD PHIL
1	NAVSHIPYD PTSMH
1	NAVSHIPYD PUG
1	CMDT, USCG
1	CO & DIR, USNEES
1	CO & DIR, USNUSL
1	CO, USNUOS, Des Sec
1	CDR, USNAVTESTCEN
1	CDR, USNWPNLAB, Dahlgren
1	CDR, USNOL, White Oak
1	CDR, USNOTS, China Lake
1	CDR, USNOTS, Pasadena Annex
4	CDR, ASTIA, Attn: TIPDR
1	DIR, USNRL
1	DIR, NASA
2	DIR, Langley Res Ctr, NASA
1	DIR, Marine Physical Lab, Scripps Inst of Ocean, Univ of Calif
2	DIR, Iowa Inst of Hydrau Res, State Univ of Iowa 1 Dr. L.A. Landweber
3	DIR, Inst for Fluid Dyn & Appl Math, Univ of Md 1 Prof. J.R. Weske 1 Dr. F.R. Hama
2	DIR, DL, SIT, Hoboken
1	DIR, ORL, Penn State
1	DIR, Robinson Model Basin, Webb Inst of Nav Arch
1	DIR, Exper Nav Tank, Dept NAME, Univ of Mich
1	DIR, Inst of Engn Res, Univ of Calif, Berkeley
1	DIR, Hydrau Lab, Colorado St Univ, Ft Collins
1	DIR, St Anthony Falls Hydrau Lab, Univ of Minn, Minneapolis
1	DIR, WHOI, Woods Hole
2	SUPSHIP, Chief Nav Arch, Elec Boat Div, Genl Dyn Corp, Groton
1	SUPT, USNAVPGSCOL
1	Admin, Maritime Admin
1	Head, Dept NAME, MIT
2	NNS & DD Co 1 Asst Nav Arch 1 Dir, Hydrau Lab
1	Chief Nav Arch, Bethlehem Steel Co, Shipbldg Div, Quincy
1	Chief Nav Arch, New York Shipbldg Corp, Camden
2	Chief, Natl Hydrau Lab, Natl BuStand
2	Hydro Lab, Attn: Exec Com, CIT, Pasadena
2	Bath Iron Works Corp, Bath 1 Mr. S.A. Dudley
1	Foster Wheeler Corp, New York
1	Gibbs & Cox, Inc, New York
1	Westinghouse Elec Corp, Philadelphia
1	Editor, Appl Mech Review, San Antonio
1	Editor, Bibliography of Tech Reports, OTS, U.S. Dept of Commerce
1	Editor, Engn Index, New York
1	Librarian, SNAME, New York
1	Librarian, Franklin Inst, Philadelphia
1	Librarian, Engn Soc Library, New York
1	Librarian, Inst of Aero Sci, New York
1	Librarian, Pacific Aero Library, IAS, Los Angeles
1	Librarian, Reed Research, Inc
8	ALUSNA
1	BSRA
1	Dir, Hydrau Lab, NRC, Ottawa, Canada
1	Dir, Bassin d'Essais des Carenes, Paris, France
1	Dir, Institut de Recherches de la Construction Navale, Paris, France
1	Dir, Nederland Scheepsbouwkundig Proefstation, Wageningen, The Netherlands
1	Dir, Institut fur Schiffbau der Universitaet Hamburg, Berliner Tor 21, Hamburg 1, Germany
2	Superintendent, Ship Div, NPL, Teddington, Middlesex, England 1 Mr. R.S. Cutland
1	Dir, Admiralty Experimental Works, Haslar, Gosport, Hampshire, England
1	Dir, Admiralty Research Laboratory, Teddington, Middlesex, England
1	Dir, Canal de Esperiencias Hidrodinamicas, El Pardo (Madrid) Spain
1	Dir, Skipsmodelltanken, Trondheim, Norway
1	Dir, Statens Skeppsprovningsanstalt, Goteborg c, Sweden
1	Librarian, NE Coast Inst of Engrs & Shipbldrs, Bolbec Hall, Newcastle Upon-Tyne, 1 England

David Taylor Model Basin. Report 1170.
BOUNDARY-LAYER INVESTIGATION ON USS TIMMERMAN (EAG 152) (EX-DD828), by Clifford L. Sayre, Jr. and Ralph J. Duerr. Aug 1960. iv, 19p. illus., photos., diagrs., tables, refs.
UNCLASSIFIED

Results of velocity measurements in the boundary layer of USS TIMMERMAN (EAG 152) are presented in this report. Measurements of velocities in the throat of the condenser scoop and the pressure drops across the condenser are also given. A generalized form of Prandtl's equation for the growth of the turbulent boundary layer on a flat plate is derived for use in estimating the boundary layer thickness at large Reynolds numbers.

1. Boundary layer – Measurement
2. Fluid flow – Velocity – Measurement
3. Ships – Boundary layer
4. TIMMERMAN (U.S. fleet ballistic missile ship EAG 152)

I. Sayre, Clifford L.
II. Duerr, Ralph J.
III. S-F013 08 08

David Taylor Model Basin. Report 1170.
BOUNDARY-LAYER INVESTIGATION ON USS TIMMERMAN (EAG 152) (EX-DD828), by Clifford L. Sayre, Jr. and Ralph J. Duerr. Aug 1960. iv, 19p. illus., photos., diagrs., tables, refs.
UNCLASSIFIED

Results of velocity measurements in the boundary layer of USS TIMMERMAN (EAG 152) are presented in this report. Measurements of velocities in the throat of the condenser scoop and the pressure drops across the condenser are also given. A generalized form of Prandtl's equation for the growth of the turbulent boundary layer on a flat plate is derived for use in estimating the boundary layer thickness at large Reynolds numbers.

1. Boundary layer – Measurement
2. Fluid flow – Velocity – Measurement
3. Ships – Boundary layer
4. TIMMERMAN (U.S. fleet ballistic missile ship EAG 152)

I. Sayre, Clifford L.
II. Duerr, Ralph J.
III. S-F013 08 08

David Taylor Model Basin. Report 1170.
BOUNDARY-LAYER INVESTIGATION ON USS TIMMERMAN (EAG 152) (EX-DD828), by Clifford L. Sayre, Jr. and Ralph J. Duerr. Aug 1960. iv, 19p. illus., photos., diagrs., tables, refs.
UNCLASSIFIED

Results of velocity measurements in the boundary layer of USS TIMMERMAN (EAG 152) are presented in this report. Measurements of velocities in the throat of the condenser scoop and the pressure drops across the condenser are also given. A generalized form of Prandtl's equation for the growth of the turbulent boundary layer on a flat plate is derived for use in estimating the boundary layer thickness at large Reynolds numbers.

1. Boundary layer – Measurement
2. Fluid flow – Velocity – Measurement
3. Ships – Boundary layer
4. TIMMERMAN (U.S. fleet ballistic missile ship EAG 152)

I. Sayre, Clifford L.
II. Duerr, Ralph J.
III. S-F013 08 08